Theoretical Study on the Aromaticity of Benzenes Annelated to Small Rings

Shogo Sakai*

Department of Information Systems Engineering, Faculty of Engineering, Osaka Sangyo University, Daito, 574-8530 Japan

Received: July 24, 2002; In Final Form: September 12, 2002

The aromaticity of benzenes annelated to small rings is studied through ab initio molecular orbital calculations. The aromaticity of benzene is defined in terms of the equivalent electronic states for six π bonds from a configuration interaction localized molecular orbital CASSCF (CiLC) analysis on the basis of ab initio calculations, and the nature of the Kekule structure is obtained based on the deviation from this aromaticity. The deviation is calculated by the CiLC method for benzenes annelated to one of three types of small rings, revealing Mills−Nixon and reverse Mills−Nixon effects. The deviation from the aromaticity is determined by the relative dominance of σ strain-induced bonds or the potential field of adjacent atoms or groups.

1. Introduction

The aromatic or Kekule structure of benzenes has been under investigation for over a century, and the role of the Mills−Nixon effect remains a contentious issue. The Mills−Nixon effect, describing the deformation of the benzene moiety when annelated to a small saturated ring, was originally proposed to explain the reactivity and selectivity of benzenes annelated to small rings. The effect itself is stated as a significant alternation of bond length within the benzene nucleus when annelated to a small ring. Diercks and Vollhardt[1] reported the synthesis and structural characterization of the first cyclohexatrienes as a star phyenylene.

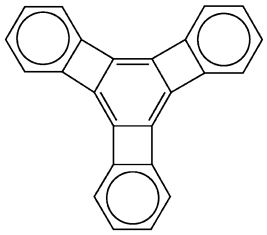

Triangular [4] phenylene

The validity of the Mills−Nixon effect for bond-localized benzenes has been examined theoretically by many researchers.[2−19] These studies can be categorized into analysis based on three broad definitions of bond localization in strained aromatic systems. One is the classic π approach,[4,5,7,18,19] which relies on aromaticity−antiaromaticity arguments to explain the phenomenon. This approach predicts that if the small ring contains $4n + 2$ electrons, the systems should exhibit longer exocyclic bonds to the annelated small ring(s) as compared to the endocyclic bonds.

In the second approach, bond localization is explained by strain-induced bond localization,[2,3,6,10,12,15,16,19] by which the strain effect causes rehybridization in the strained atoms. Stanger and Vollhardt[2] simulated artificially distorted benzene (Figure 1) in order to demonstrate strain-induced bond localization by calculating the structure of the benzene with a fixed HCC bonding angle (θ) (the D_{3h} symmetry). The calculated structure revealed the bond localization of C−C: for $\theta = 90°$ (fixed), $R_1 = 1.3463$ Å and $R_2 = 1.5790$ Å at the MP2/3-21G level and $R_1 = 1.3288$ Å and $R_2 = 1.5290$ Å at the HF/6-31G* level. The last approach deals with the curvature of the bonds involved.[10]

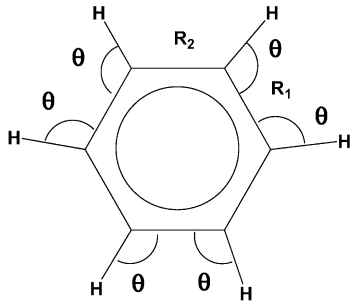

Figure 1. Model of artificially distorted benzene.

CHART 1

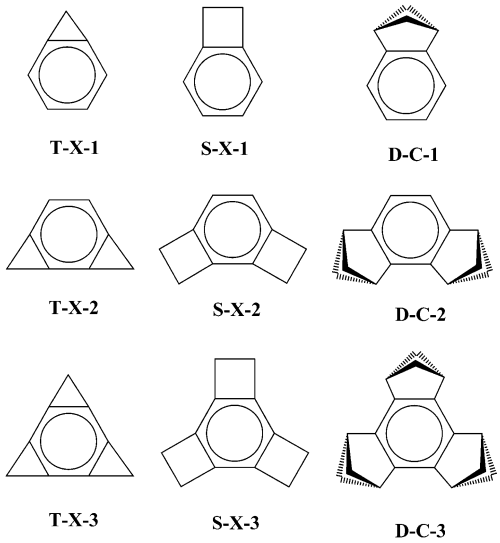

* To whom correspondence should be addressed. E-mail: sakai@ise.osaka-sandai.ac.jp.

10.1021/jp021722a CCC: $22.00
Published on Web 11/06/2002

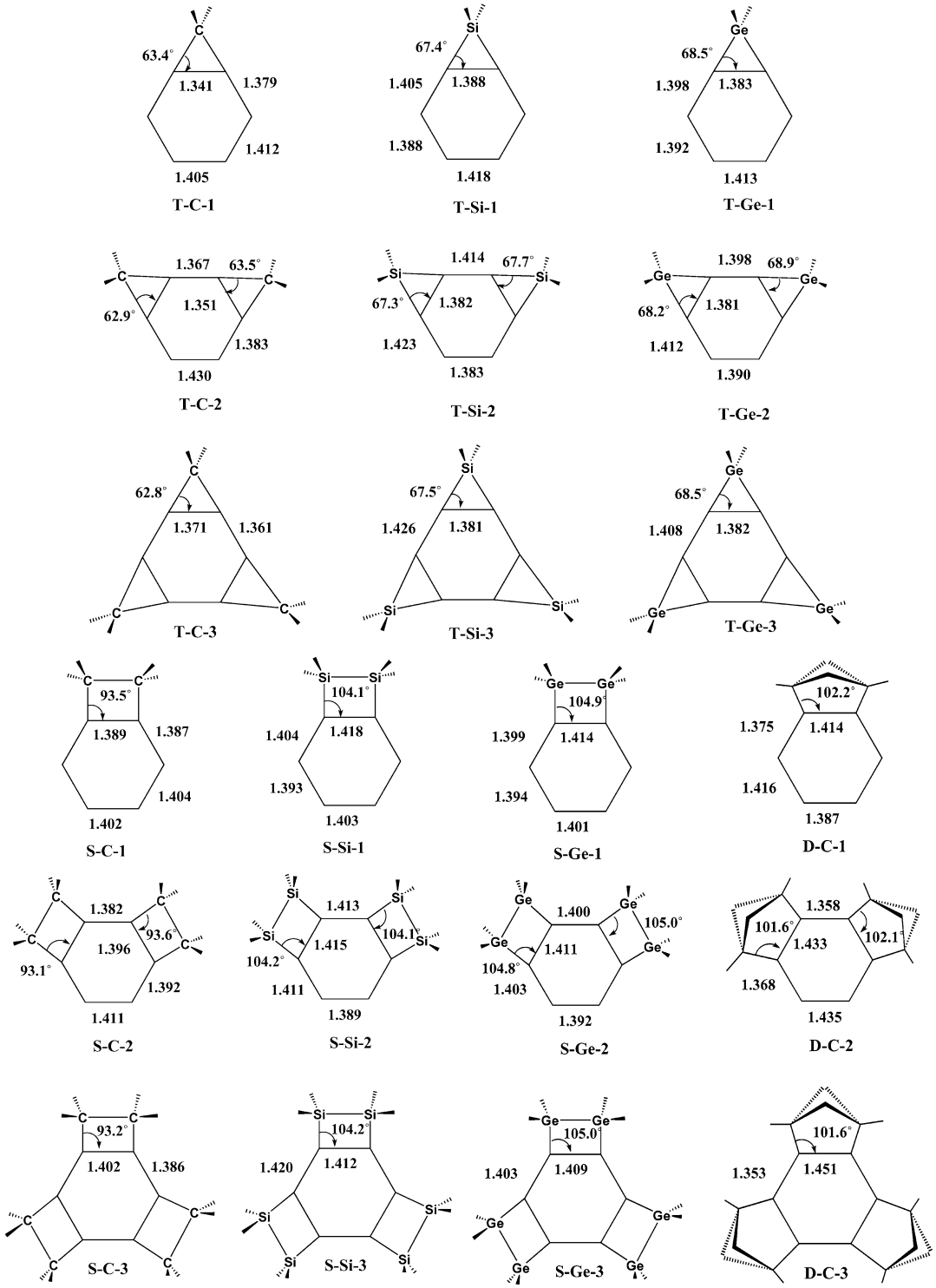

Figure 2. Stationary point geometries for benzenes annelated to small rings by CASSCF(6,6)/6-31G(d).

In this approach, the index ΔR is employed, representing the difference between the exocyclic and the endocyclic C−C bond lengths in the benzene ring annelated to small rings. However, the difference in bond lengths does not always explain the bond localization. In particular, a π bond often exhibits bond localization by the influence of the potential field in the neighborhood.

In the previous paper,[20] we defined the aromaticity of benzene type by ab initio molecular orbital (MO) calculations for the case that the weights of electronic states for six π electrons bonds were equivalent for each C−C bond. In this instance, bond localization can be considered to be the deviation from aromaticity. In the present paper, we report the bond localization, or the deviation from aromaticity, for benzenes annelated to one of three types of small rings as displayed in Chart 1.

2. Computational Methods

All equilibrium geometries were determined with analytically calculated energy gradients using a complete active space (CAS) self-consistent field (SCF) method[21] with the 6-31G(d) basis set.[22] For the CASSCF calculation, six active spaces corresponding to three π and π^* orbitals for benzenes rings were

TABLE 1: Difference between Longest and Shortest C−C Bond Lengths (Δ*R*) for T-XC-*n* and S-X-*n* Series

	C	Si	Ge
T-X-1	0.071	0.030	0.030
T-X-2	0.079	0.041	0.031
T-X-3	0.010	0.045	0.026
S-X-1	0.015	0.025	0.020
S-X-2	0.029	0.026	0.019
S-X-3	0.016	0.008	0.006
D-X-1	0.041		
D-X-2	0.075		
D-X-3	0.098		

included, and all configurations in the active spaces were generated.

To interpret the aromaticity, a configuration interaction (CI) localized molecular orbital (LMO) CASSCF (CiLC) analysis was carried out according to a method described in detail elsewhere[20,23−33] using the 6-31G(d) basis set. In this procedure, the CASSCF is calculated to obtain a starting set of orbitals for the localization procedure, after which the six CASSCF-optimized orbitals are localized by the Boys localization procedure.[34] The calculated localized orbitals are very atomic in nature and appear as the p_π orbital of a carbon atom. Using the localized MOs as a basis, a full CI with determinant level is performed to generate electronic structures and their relative weights in the atomic orbital-like wave functions. The total energy as calculated by the CI procedure corresponds to that by the CASSCF calculation, and the relative weights of the electronic states of different CI configurations are expected to indicate the electronic bond state. This procedure is referred to as the CiLC method.

Calculations for the CiLC method were performed using the GAMESS software package.[35] Other calculations were carried out using Gaussian98.[36]

3. Results and Discussion

3.1. Geometry. The stationary point geometries for benzenes annelated to one of the three types of small ring(s) (three-membered, four-membered, and bicyclic rings) treated here are shown in Figure 2. The notation A-X-*n* is adopted for this annelation, where A = T, S, or D, which refers to the three-membered, four-membered, and bicyclic rings, respectively; X indicates the element of the small ring; and *n* is the number of annelated small rings.

For benzenes annelated to a three-membered ring, the length of the C−C bond (endo) of the annelation of CH_2 and that of the adjacent bond (exo) for monosubstitution are shorter by 0.055 and 0.017 Å than those of benzene, respectively. As more three-membered rings (CH_2) are annelated, the C−C endo bond lengths increase and the C−C exo bonds decrease. As a result, the C−C endo bond is longer than the exo bond in T-C-3.

For the three-membered rings SiH_2 and GeH_2, the C−C endo bond length remains largely unchanged with any increase in the number of annelations, whereas the adjacent bond (exo) becomes shorter. Consequently, the exo bonds are longer than the endo bonds for T-Si-3 and T-Ge-3, which is the reverse of the situation predicted by the Mills−Nixon effect.[6] Similar variations in bond lengths are observed for the four-membered and bicyclic rings.

For each X of the T-X-n series, the angle between XH_2 and the C−C bond of benzene ring remains largely unchanged with any increase in the number of annelations. The angle for X = C is a little smaller than those of X = Si and Ge. However, the ariation of the angle for these compounds does not correlate to the C−C endo−exo bond lengths. A similar relation in the angle is obtained for the four-membered and bicyclic rings.

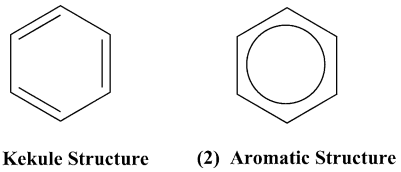

(1) Kekule Structure (2) Aromatic Structure

Figure 3. Kekule structure and aromatic structure for benzene.

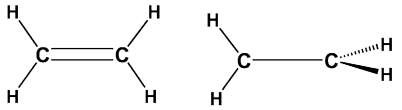

(3) Ethylene (4) Twisted Ethylene

Figure 4. Ethylene and twisted ethylene.

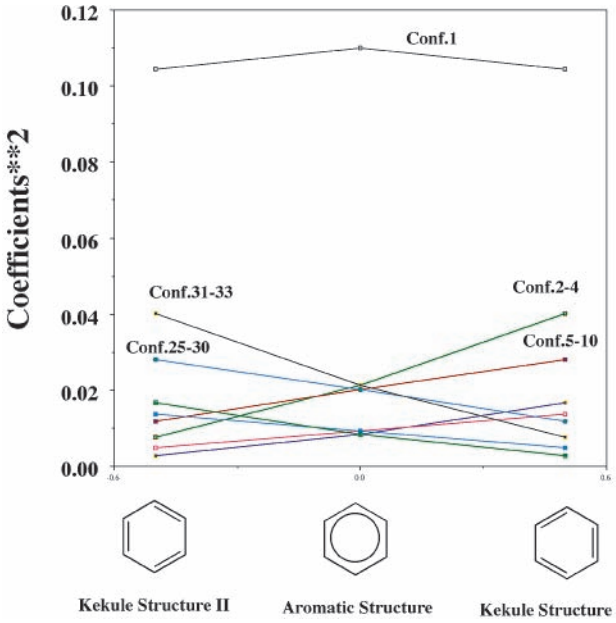

Figure 5. Weights of CI coefficients by CiLC calculations for aromatic and Kekule structure.

The differences Δ*R* between the longest C−C bond length and the shortest C−C bond length in the benzene rings are listed in Table 1. In the T-C-*n* series, the Δ*R* of T-C-2 and T-C-1 are larger than that of T-C-3, and that of S-C-2 is largest in the S-C-*n* series. In the D-C-*n* series, Δ*R* increases with the number of annelated rings. For the T-X-*n* series, the values of Δ*R* for the C rings are larger than those for Si and Ge, except when three rings are annelated. Therefore, if the aromaticity and Kekule nature were determined from the geometry parameters, T-C-1 and T-C-2 would exhibit the largest deviation from aromaticity in the T-X-*n* series. However, this contradicts the Mills−Nixon hypothesis. Therefore, the discussion of the aromaticity and Kekule nature of these compounds will be redirected to an analysis of the electronic states of bonds.

3.2. Aromaticity. The aromaticity and Kekule structures of benzene were characterized by CiLC analysis using the 6-31G-(d,p) basis set in our previous paper.[20] The results are outlined briefly in the following for comparison with the present results. Both the Kekule structure and the aromatic structure are examined here for a basic benzene (Figure 3), using the C═C double bond length for ethylene (1.338 Å) and the C−C bond length for twisted ethylene (1.469 Å) for the respective bonds in the Kekule structure (Figure 4).

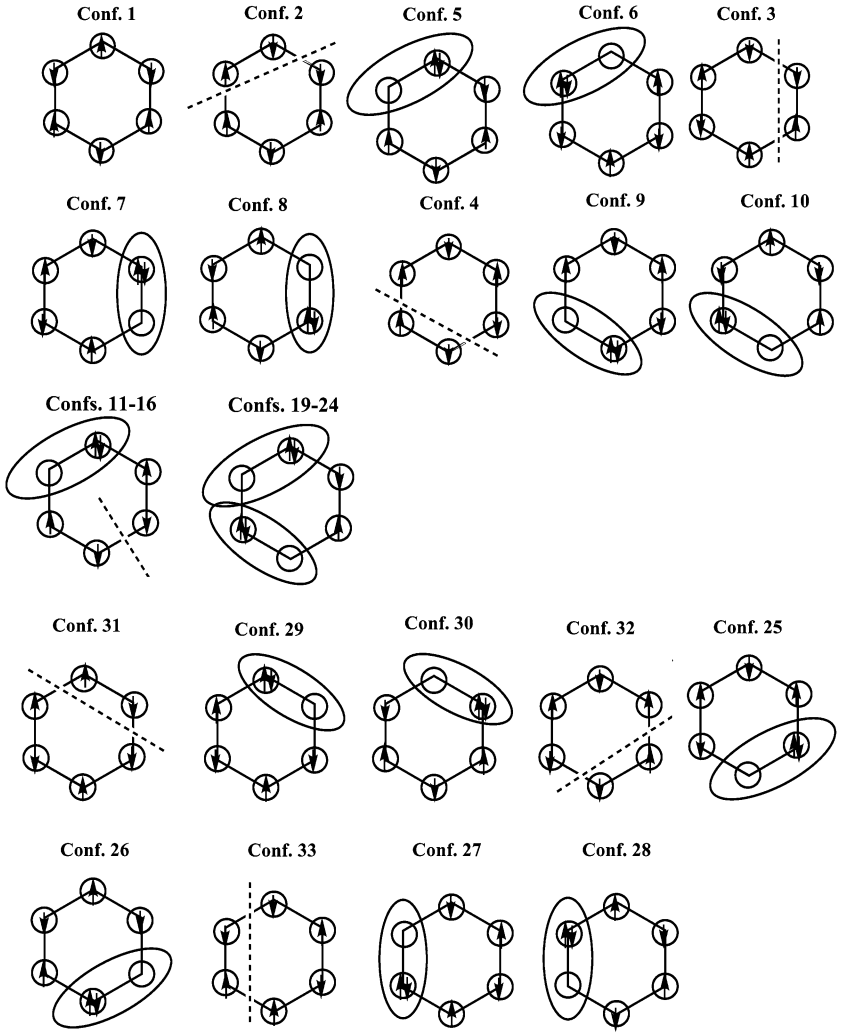

Figure 6. Selected electronic configurations of benzene for CiLC analysis. Dotted lines denote triplet coupling (antibonding) between orbitals, and ellipses denote ionic coupling.

The geometry parameters of benzene, ethylene, and twisted ethylene were optimized by CASSCF calculation based on the 6-31G(d) basis set. CiLC calculations were performed for the Kekule and aromatic benzene structures. The squares of the CI coefficients obtained by the CiLC method are shown in Figure 5. Small values (<0.01) for both structures are neglected. Some configurations for the larger CI coefficients are shown in Figure 6. The weight of configuration 1, the reference state, remains virtually unchanged between the aromatic and the Kekule structures, whereas the weights of Kekule structure I for configurations 2−10 are higher and those for configurations 25−33 are lower. The total weight for configurations 2−33 is therefore similar to that for the aromatic structure. Configurations 2−4 are considered to involve the interaction of singlet couplings in the double bonds of Kekule structure I, and configurations 5−10 are associated with polarization of the double bond part of Kekule structure I. Configurations 2−10 may therefore represent overall bonding via the double bond parts of Kekule structure I. In fact, the π bonding of ethylene can be described as the singlet coupling between p_π orbitals and the polarization terms (Figure 7).

On the other hand, configurations 25−33 are attributed to bonding via the single bond parts of Kekule structure I. Configurations 11−24 are expected to represent higher order excitation terms. On the basis of the above results, the aromatic

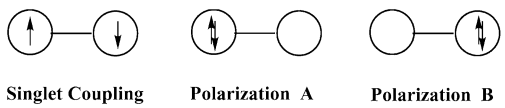

Figure 7. Electronic configurations of ethylene.

structure of benzene can be described in terms of equivalent singlet coupling and polarization terms for all six bonds.

3.3. CiLC Analysis. The squared CI coefficients (weights of configurations) for nine compounds (S-C-*n*, T-C-*n*, and D-C-*n*; $n = 1-3$) as determined by CiLC analysis are shown in Figure 8. The largest weight (top line in figure) for each compound is that of configuration 1. The next largest group of weights (for T-C-*n* and S-C-*n*) corresponds to configurations 2−10 and 25−33, and the smallest group includes configurations 11−16 and 19−24. The CI coefficients for S-C-*n* ($n = 1-3$) are almost the same as those of the aromatic benzene, indicating that benzenes annelated to four-membered ring(s) exhibit aromatic nature. The largest, the next largest, and the smallest weights groups for S-C-*n* correspond to those of the aromatic benzene of the center in Figure 5. As shown in the previous section, the difference of the aromatic and the Kekule character can be seen in the dispersion of the weights of configurations in the second largest group. For T-C-*n* and D-C-*n* ($n = 1-3$), the Kekule character becomes remarkable and more so with

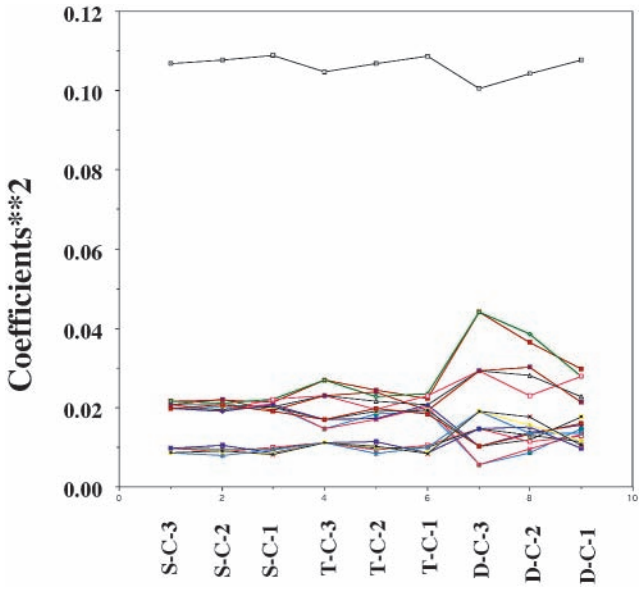

Figure 8. Weights of CI coefficients by CiLC calculation for S-C-*n*, T-C-*n*, and D-C-*n* series.

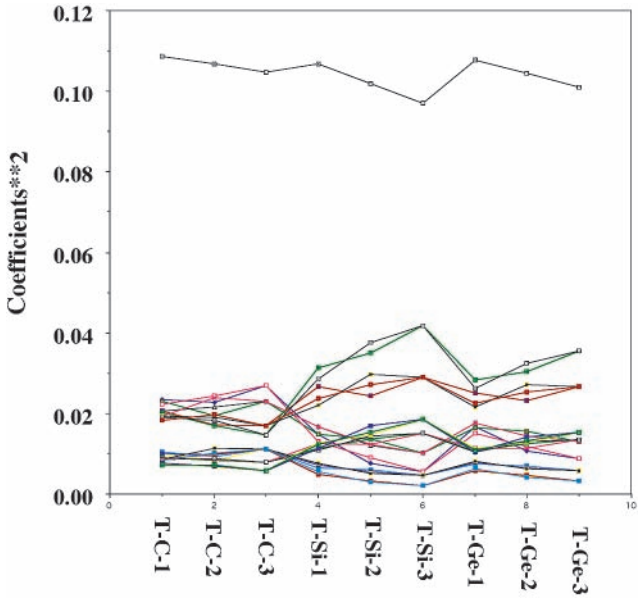

Figure 9. Weights of CI coefficients by CiLC calculation for T-X-*n* series.

increasing *n*. For T-C-*n*, the largest difference (ΔR) in the C−C bond distances is that of T-C-2 (0.079 Å). However, on the basis of the weights of electronic state for the C−C bonds, T-C-3 exhibits greater deviation from aromaticity than either T-C-2 or T-C-1. The deviation is also greater than that for S-C-3, while the ΔR of S-C-3 is slightly larger. This implies that the C−C bond distances are not a good index for differentiating aromatic and Kekule character.

The squared CI coefficients for the T-X-*n* series are shown in Figure 9. The T-Si-*n* series exhibits a significantly stronger Kekule structure as compared to the T-C-*n* series. In the figure, it can be seen that the weights for the double bond and single bond configurations of the T-C-*n* series occur in a different order than in the T-Si-*n* and T-Ge-*n* series, indicating a reversing of the Mills−Nixon effect for those two series, although the effect is less pronounced for the T-Ge-*n* series due to the weaker Kekule character.

TABLE 2: Weights of CI Coefficients by CiLC Calculation for Six Compounds and Three Benzenes[a]

	exo			endo			exo−endo
	singlet	polar	total	singlet	polar	total	difference
T-C-3	0.027	0.046	0.073	0.015	0.034	0.049	0.024
T-Si-3	0.006	0.020	0.026	0.042	0.058	0.100	−0.074
T-Ge-3	0.009	0.026	0.035	0.036	0.054	0.089	−0.054
S-C-3	0.022	0.041	0.063	0.020	0.039	0.059	0.004
S-Si-3	0.013	0.032	0.045	0.031	0.049	0.080	−0.035
D-C-3	0.044	0.059	0.103	0.006	0.020	0.026	0.077
ben (D_{6h})[b]	0.021	0.040	0.062	0.021	0.040	0.062	0.000
ben (D_{3h})[c]	0.040	0.056	0.096	0.008	0.024	0.031	0.065
ben (90)[d]	0.049	0.060	0.109	0.005	0.018	0.023	0.086

[a] Singlet refers to singlet coupling of C−C bonds, and polar refers to the polarization term and includes both polarizations A and B. [b] Aromatic benzene. [c] Kekule benzene. [d] Benzene structure optimized with C−C−H angle of 90°.

TABLE 3: Weight of CI Coefficients by CiLC Calculation for A-X-3 Series and Artificially Distorted D_{6h} Benzene

	exo			endo			exo−endo
	singlet	polar	total	singlet	polar	total	difference
T-C-3	0.027	0.046	0.073	0.016	0.036	0.052	0.021
T-Si-3	0.008	0.026	0.033	0.036	0.054	0.090	−0.057
S-C-3	0.020	0.039	0.059	0.022	0.042	0.064	−0.005
S-Si-3	0.014	0.033	0.047	0.028	0.047	0.076	−0.029
D-C-3	0.030	0.048	0.078	0.014	0.032	0.046	0.032
ben (90, D_{6h})	0.025	0.044	0.069	0.018	0.037	0.055	0.014

The squared CI coefficients for the C−C bonds of the exo and endo positions are listed in Table 2. The weights for the artificially distorted benzene (HCC bonding angle = 90°: ben $(90))^2$ are also shown in order to demonstrate strain-induced bond localization. A positive difference between the exo and the endo coefficients indicates the Mills−Nixon effect, and negative values indicate the reverse Mills−Nixon effect. The exo−endo weight for T-Si-3 is reversed to that for D-C-3 (Kekule structure). The weight for the singlet term at smaller total weights is smaller than half the polarization term (equivalent structure in polarization configuration) and larger than half the polarization at larger total weights. This relationship holds for all of the compounds examined here, including dissimilar compounds. For example, the exo weights for T-Si-3 are identical to the endo weights for D-C-3.

The CiLC analysis therefore highlights the difference between exo and endo bond characters. The CiLC analysis in Table 2 was performed for the equilibrium (stationary point) geometries. Further calculations were subsequently performed on six compounds with accurate C−C bond length for D_{6h} symmetry in order to identify the key characteristics of the π bonds in benzene annelation. In this configuration, the C−C bonds are 1.396 Å in length for both exo and endo positions and all compounds. The squared CI coefficients are listed in Table 3, including those for the distorted benzenes. The exo−endo difference for ben(90, D_{6h}) is dramatically smaller than that for ben (90). The higher value for ben (90) is therefore attributed to the difference in the lengths between the C−C exo and the C−C endo bonds. The potential field of the σ bond frame affects only few for the polarity of π bonds with respect to bond localization. In the constrained T-C-3 structure, the exo−endo difference is only slightly larger than that for ben (90, D_{6h}). The bond alternation for T-C-3 is therefore thought to originate from the σ bond-induced localization of the C−C−C bond angle. Although the negative exo−endo difference for T-Si-3 indicates the reverse Mills−Nixon effect, the bond alternation due to the σ bond-induced effects of the Si−C−C bond angle suggests a positive Mills−Nixon effect. This can be explained

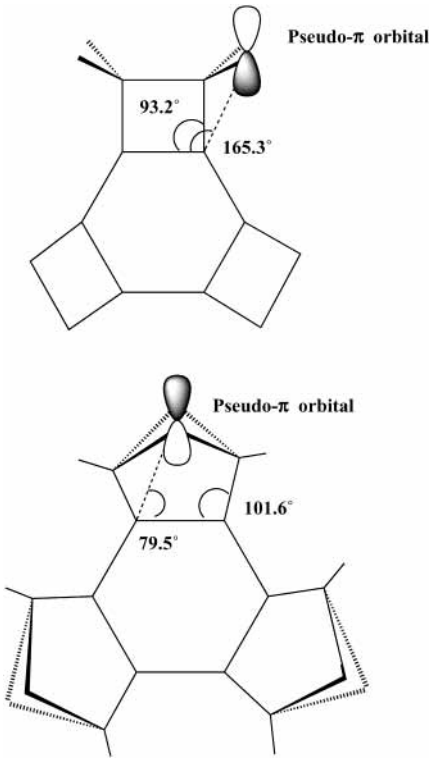

Figure 10. Pseudo-π orbitals for S-X-3 and D-X-3.

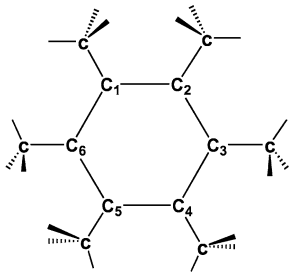

Figure 11. Structure of hexamethyl benzene with D_{3h} symmetry.

by the dominance of electrostatic effects on π bonds by SiH_2, overriding any bond alternation as a result of σ bond-induced effects. This situation is also observed for S-Si-3. A comparison between S-C-3 and D-C-3 reveals very interesting information with regard to bond alternation. The exo−endo differences for S-C-3 and D-C-3 contradict the results predicted by σ strained-induced effects from the bond angle. However, the results for S-C-3 and D-C-3 can be explained by the direction (or angle) for the pseudo-π orbital, which is similar to that of a methyl group. For S-C-3, the σ orbitals of two C−H bonds of CH_2 can be considered to be pseudo-π orbitals, and when the center of such an orbital corresponds to the midpoint between two H atoms, the angle of the pseudo-π orbital and the C−C bond of the endo position is 165°, significantly exceeding the 120° of the equilibrium structure. In the same way, two σ orbitals of the C−C bonds in the bicyclic configuration of D-C-3 can be considered to be pseudo-π orbitals. In this case, the angle between the pseudo-π orbital and the endo C−C bond will be about 80°.

We can now explain the difference in bond alternation between S-C-3 and D-C-3, assuming the validity of pseudo-π orbitals (Figure 10). When the geometry of hexamethyl benzene D_{3h} (Figure 11) is optimized at the B3LYP/6-31G(d) level, the length of the C_1-C_2 bond is about 0.014 Å longer than that of the C_2-C_3 bond.

4. Conclusion

The aromaticity of benzenes annelated to three kinds of small rings was studied through ab initio MO calculations. The difference in bond distances between the largest and the smallest C−C bonds in the benzene ring was found to not to correlate consistently with the Mills−Nixon hypothesis. The aromaticy and Kekule structures of benzene were discussed based on ab initio MO calculations with electronic states for each C−C bond obtained by CiLC analysis. The deviation from aromaticity was determined through CiLC calculations for benzenes annelated to small rings and artificially distorted benzenes ($\theta = 90°$). The difference between the square of the CI coefficients for exo and endo C−C bonds was found to indicate whether the Mills−Nixon effect was positive or reversed, and the deviation from aromaticity was determined by the dominance of σ bond-induced effects or potential field effects on π bonds.

Acknowledgment. This research was supported by a Grant-in-Aid for Scientific Research from the Ministry of Education, Science and Culture of Japan. Computer time was made available by the Computer Center of the Institute for Molecular Science and Osaka Sangyo University using the SGI Power Challenge computer.

References and Notes

(1) Diercks, R.; Vollhardt, K. P. C. *J. Am. Chem. Soc.* **1986**, *108*, 3150.
(2) Stanger, A.; Vollhardt, K. P. C. *J. Org. Chem.* **1988**, *53*, 4889.
(3) Stanger A. *J. Am. Chem. Soc.* **1991**, *113*, 8277.
(4) Baldridge, K. K.; Siegel, J. S. *J. Am. Chem. Soc*. **1992**, *114*, 9583.
(5) Faust, R.; Glendening, E. D.; Streitwieser, A.; Vollhardt, K. P. C. *J. Am. Chem. Soc*. **1992**, *114*, 8263.
(6) Maksic, Z. B.; Eckert-Maksic, M.; Pfeifer, K.-H. *J. Mol. Struct.* **1993**, *300*, 445.
(7) Baldridge, K. K.; Siegel, J. S. *J. Am. Chem. Soc.* **1993**, *115*, 10782.
(8) Siegel, J. S. *Angew. Chem., Int. Ed. Engl.* **1994**, *33*, 1721.
(9) Ou, M.-C.; Chu, S.-Y. *J. Phys. Chem.* **1994**, *98*, 1087.
(10) Yanez, O. M. M.; Ecker-Maksic, M.; Muksic, Z. B. *J. Org. Chem.* **1995**, *60*, 1638.
(11) Frank, N. L.; Baldridge, K. K.; Siegel, J. S. *J. Am. Chem. Soc.* **1995**, *117*, 2102.
(12) Burgi, H.-B.; Baldridge, K. K.; Hardcastle, K.; Frank, N. L.; Gantzel, P.; Siegel, J. S.; Ziller, J. *Angew. Chem., Int. Ed. Engl.* **1995**, *34*, 1454.
(13) Cardullo, F.; Giuffrida, D.; Kohnke, F. H.; Raymo, F. M.; Stoddart, J. F.; Williams, D. J. *Angew. Chem., Int. Ed. Engl.* **1996**, *33*, 339.
(14) Jemmis, E. D.; Kiran, B. *J. Org. Chem.* **1996**, *61*, 9006.
(15) Eckert-Maksic, M.; Glasovac, Z.; Maksic, Z. B.; Zrinski, I. *THEOCHEM* **1996**, *366*, 173.
(16) Mitchell, R. H.; Chen, Y.; Iyer, V. S.; Lau, D. Y. K.; Baldridge, K. K.; Siegel, J. S. *J. Am. Chem. Soc*. **1996**, *118*, 2907.
(17) Shaik, S.; Shurki, A.; Danovich, D.; Hiberty, P. C. *THEOCHEM* **1997**, *398*−*399*, 155.
(18) Stanger, A. *J. Am. Chem. Soc*. **1998**, *120*, 12034.
(19) Eckert-Maksic, M.; Glasovac, Z.; Coumbassa, N. N.; Maksic, Z. B. *J. Chem. Soc., Perkin Trans. 2* **2001**, 1091.
(20) Sakai, S. *J. Phys. Chem. A* **2000**, *104*, 922.
(21) Roos, B. In *Advances in Chemical Physics*; Lawley, K. P., Ed.; Wiley: New York, 1987; Vol. 69, Part II, p 399.
(22) Hariharan, P. C.; Pople, J. A. *Theor. Chim. Acta* **1973**, *28*, 213.
(23) Cundari, T. R.; Gordon, M. S. *J. Am. Chem. Soc.* **1991**, *113*, 5231.
(24) Sakai, S. *J. Phys. Chem. A* **1997**, *101*, 1140.
(25) Sakai, S. *Int. J. Quantum Chem*. **1998**, *70*, 291.
(26) Nguyen, M. T.; Chandra, A. K.; Sakai, S.; Morokuma, M. *J. Org. Chem.* **1999**, *64*, 65.
(27) Sakai, S. *J. Mol. Struct. (THEOCHEM)* **1999**, *461*−*462*, 283.
(28) Sakai, S.; Takane, S. *J. Phys. Chem. A* **1999**, *103*, 2878.
(29) Sakai, S. *J. Phys. Chem. A* **2000**, *104*, 922.
(30) Sakai, S. *Int. J. Quantum Chem.* **2000**, *80*, 1099.
(31) Sakai, S. *J. Phys. Chem. A* **2000**, *104*, 11615.
(32) Sakai, S. *J. Mol. Struct. (THEOCHEM)*, in press.
(33) Sakai, S. *Int. J. Quantum Chem*., in press.
(34) Foster, J. M.; Boys, S. F. *Rev. Mod. Phys*. **1960**, *32*, 300.

(35) Schmidt, M. W.; Buldridge, K. K.; Boatz, J. A.; Jensen, J. H.; Koseki, Gordon, M. S.; Nguyen, K. A.; Windus, T. L.; Elbert, S. T. *QCPE Bull.* **1990**, *10*, 52.

(36) Frisch, K. J.; Trucks, G. W.; Schlegel, H. B.; Gill, P. M. W.; Johnson, B. G.; Robb, M. A.; Cheseman, J. R.; Keith, T. A.; Petersson, G. A.; Montgomery, J. A.; Raghavachari, K.; Al-Laham, M. A.; Zakrzewski, V. G.; Ortiz, J. V.; Foresman, J. B.; Cislowski, J.; Stefanov, B. B.; Nanayakkara, A.; Challacombe, M.; Peng, C. Y.; Ayala, P. Y.; Chen, W.; Wong, M. W.; Andres, J. L.; Replogle, E. S.; Comperts, R.; Martin, R. L.; Fox, D. J.; Binkley, J. S.; DeFrees, D. J.; Baker, J.; Stewart, J. P.; Head-Gordon, M.; Gonzalez, C.; Pople, J. A. *GAUSSIAN 98*; Gaussian, Inc.: Pittsburgh, PA, 1998.